# Extended Data Figure 1

LC-MS of purified VHHs and VHH-antigen adducts.

Extended Data Figure 2
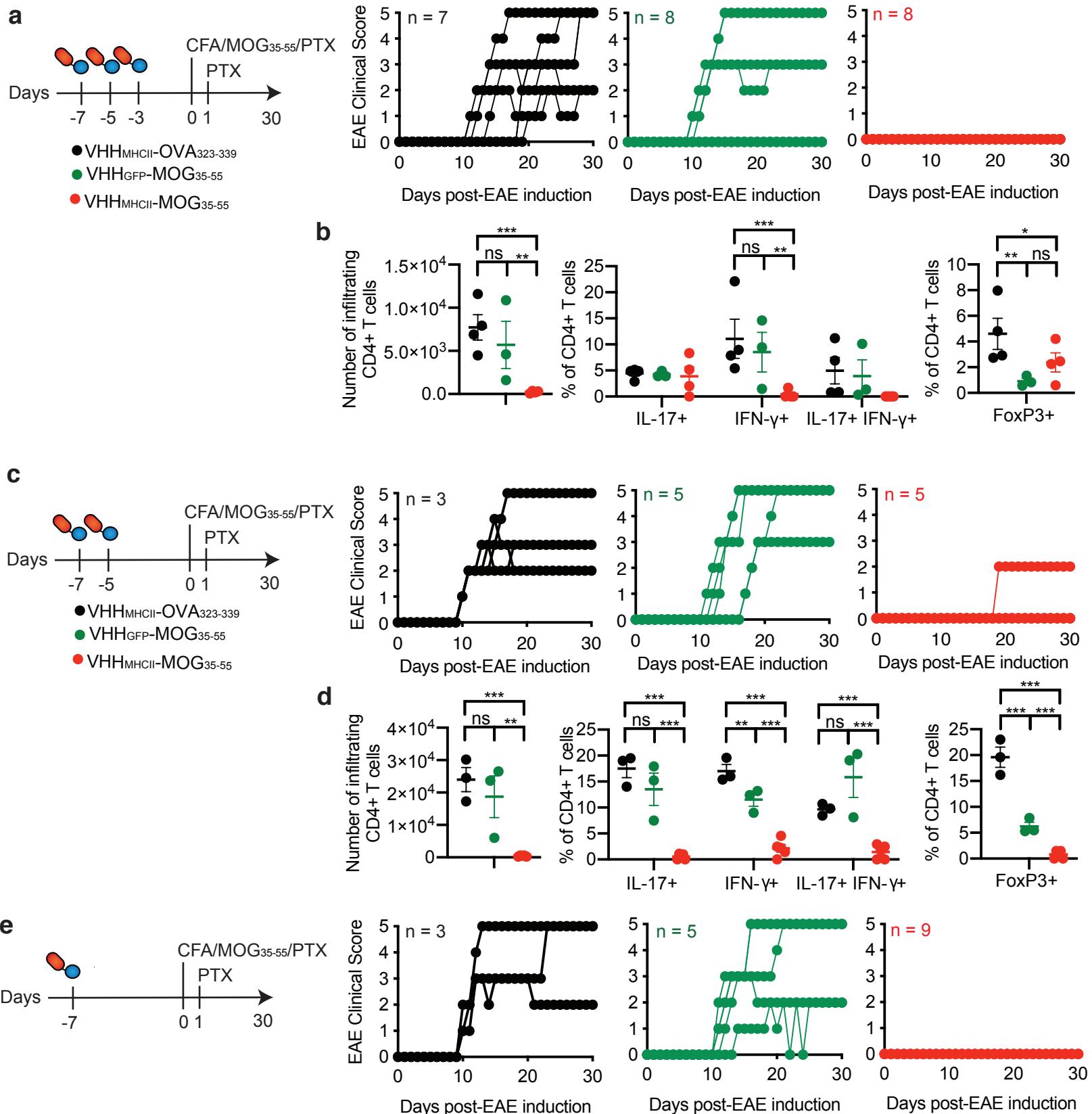
Individual clinical score of each that received VHH-peptide prophylactic treatment at (a) 3, (c) 2, and (e) 1 dose(s) as indicated. Clinical scores: 1, limp tail; 2, partial hind leg paralysis; 3, complete hind leg paralysis; 4, complete hind and partial front leg paralysis; and 5, moribund. Flow cytometry analyses of Th1 and Th17 infiltrating CD4+ lymphocytes in the spinal cord at the end point for mice that received 3 (b) and 2 (d) doses of VHH-antigen. Frequency of FoxP3+ CD4+ regulatory T cells are also indicated. Data shown as mean +/- SEM. n.s. not significant; *p<0.05, **p<0.01, ***p<0.001, unpaired t test with Holm-Sidak adjustment.

Extended Data Figure 3

a
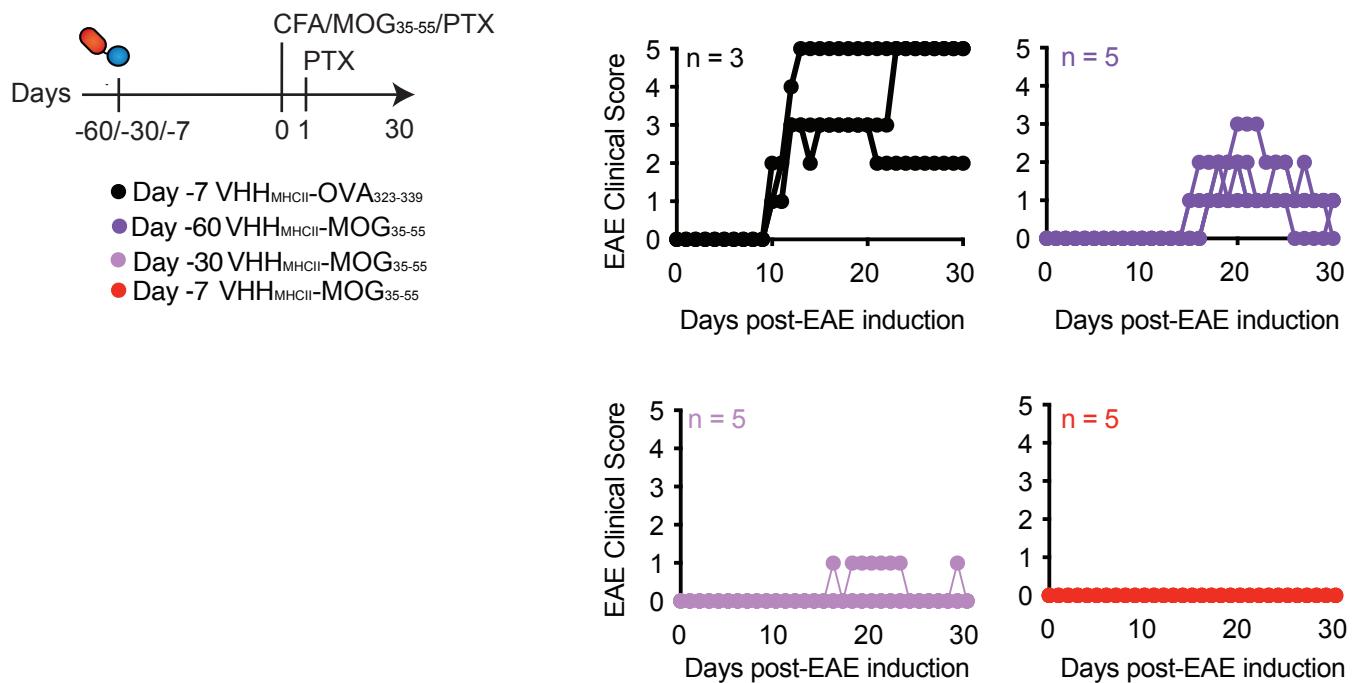
b
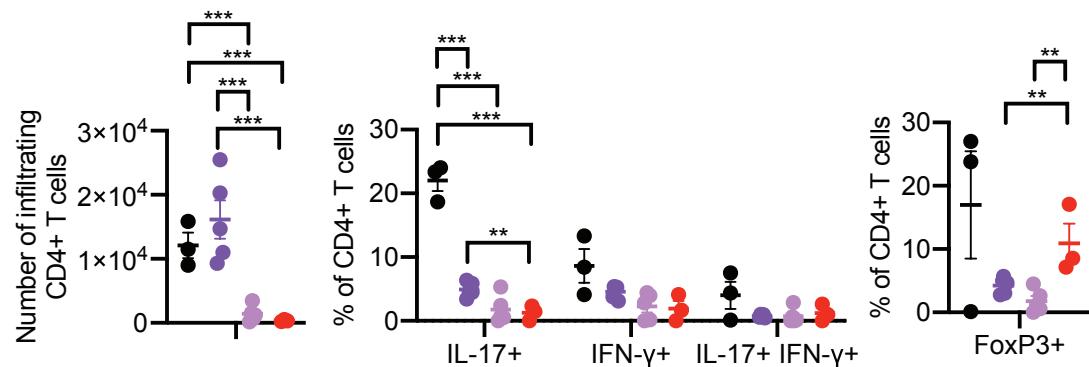
a, Individual clinical score of each that received VHH-peptide prophylactic treatment at -60, -30, and -7 days prior to EAE induction. Clinical scores: 1, limp tail; 2, partial hind leg paralysis; 3, complete hind leg paralysis; 4, complete hind and partial front leg paralysis; and 5, moribund. **b**, Flow cytometry analyses of Th1 and Th17 infiltrating CD4+ lymphocytes in the spinal cord at the end point for mice that received 1 dose of VHH-antigen at the indicated time points. Frequency of FoxP3+ CD4+ regulatory T cells are also indicated. Data shown as mean +/- SEM. n.s. not significant; *p<0.05, **p<0.01, ***p<0.001, unpaired t test with Holm-Sidak adjustment.

Extended Data Figure 4

Flow cytometry analyses of infiltrating CD4+ lymphocytes in the spinal cord at the end point for mice that received 1 dose of VHH-antigen followed by exposure to to multiple EAE challenges. Data shown as mean +/- SEM.

Extended Data Figure 5

a
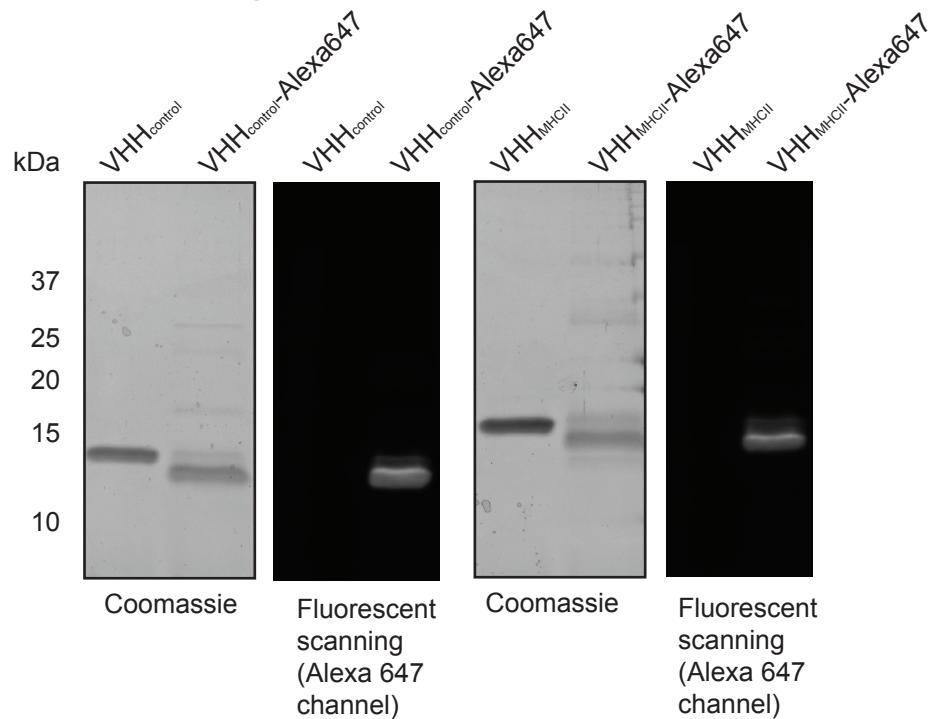
b
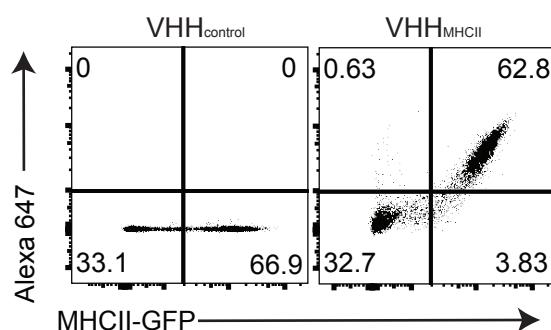
In vitro characterization of VHH-fluorophore, i.e. VHH$_{MHCII}$-Alexa 647 and VHH$_{control}$-Alexa 647. **a**, Coomassie and fluorescent western blots of unmodified and modified VHHs carrying Alexa 647 generated by sortagging. **b**, Flow cytometry analyses of splenocytes from MHCII-GFP mouse indicate positive correlation of VHH$_{MHCII}$ binding and MHCII expression.

Extended Data Figure 6
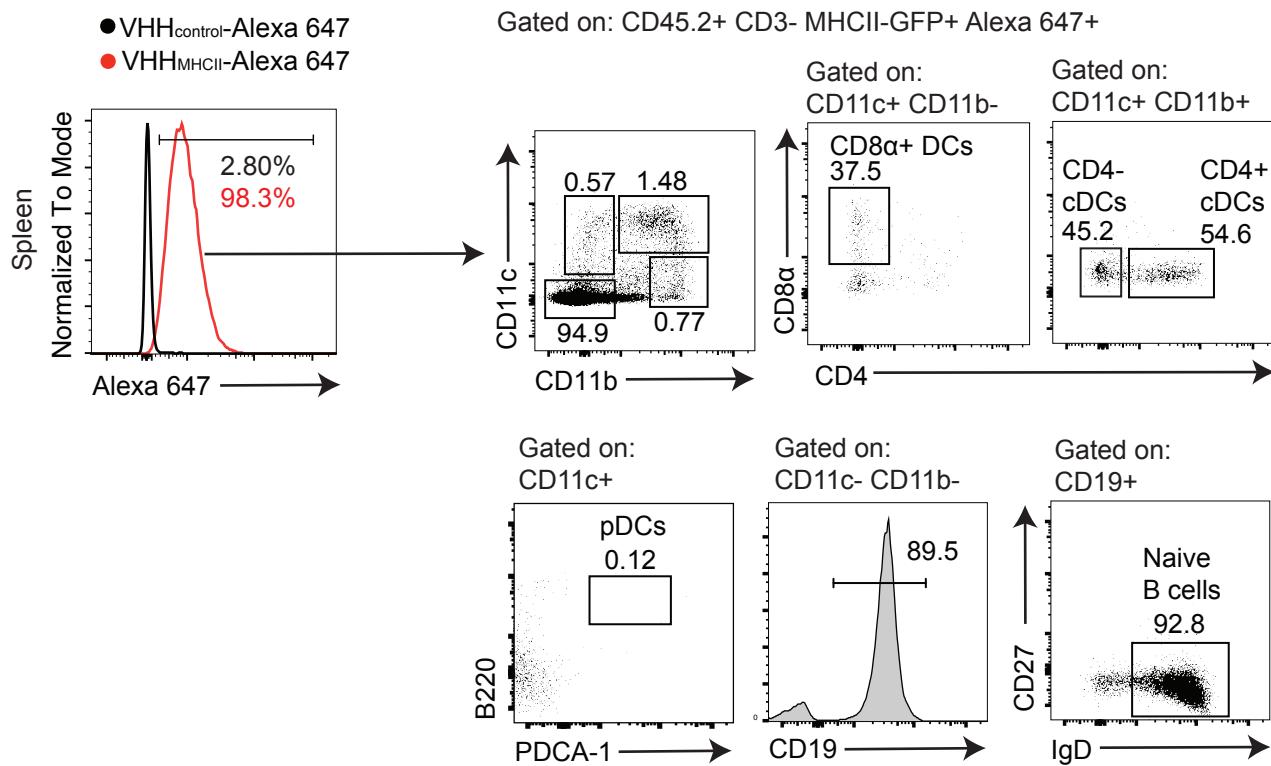
In vivo biodistribution of VHH$_{MHCII}$. VHH$_{MHCII}$-Alexa 647 was intravenously injected into MHCII-GFP mice. At 1.5 hours post injection, spleens, inguinal lymph nodes, and blood were collected and analyzed by flow cytometry. We also further dissected the subpopulation of splenic GFP+ Alexa 647+ APCs. cDCs (conventional DCs); pDCs (plasmacytoid DCs).

Extended Data Figure 7
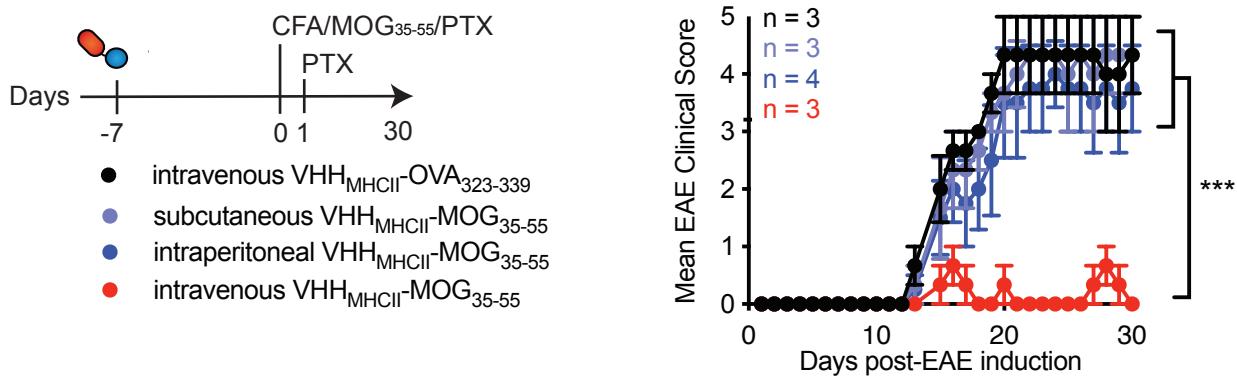
Determination whether the mode of delivery affects the VHH$_{MHCII}$-MOG$_{35-55}$ mediated protection in EAE. Mean clinical scores of mice that received VHH-peptide prophylactic treatment injected intravenously, intraperitoneally, or subcutaneously. Clinical scores: 1, limp tail; 2, partial hind leg paralysis; 3, complete hind leg paralysis; 4, complete hind and partial front leg paralysis; and 5, moribund. ***, $p < 0.01$, two-way analysis of variance (ANOVA) with repeated measures.

Extended Data Figure 8
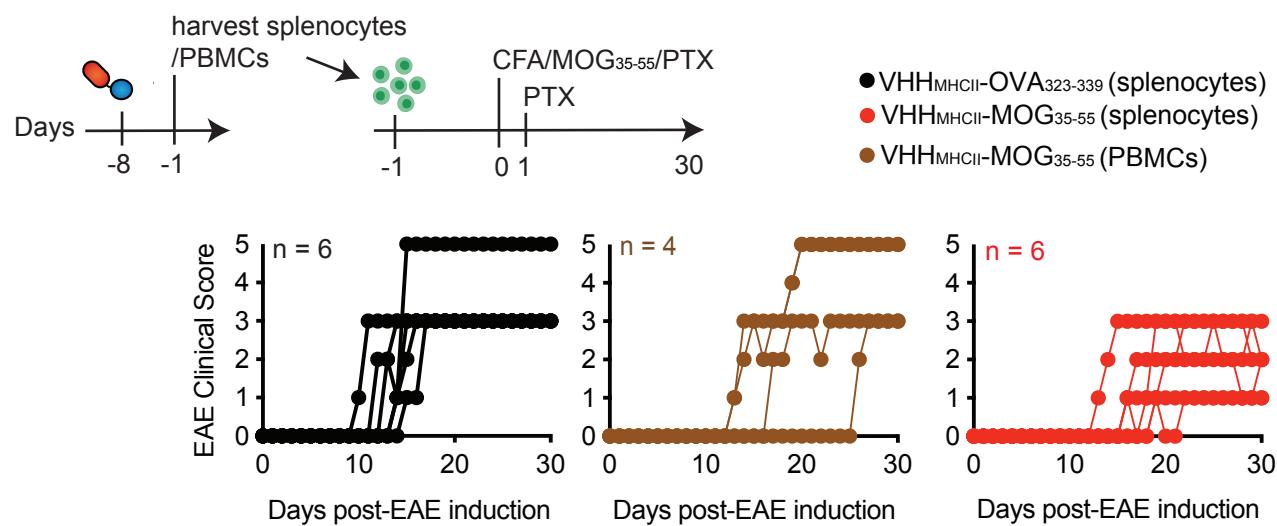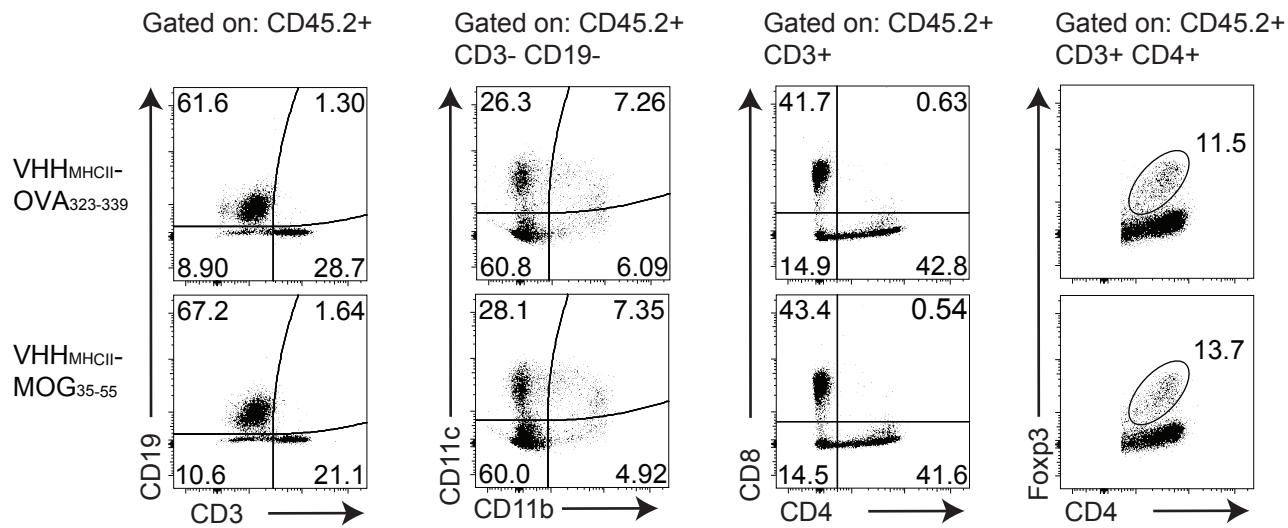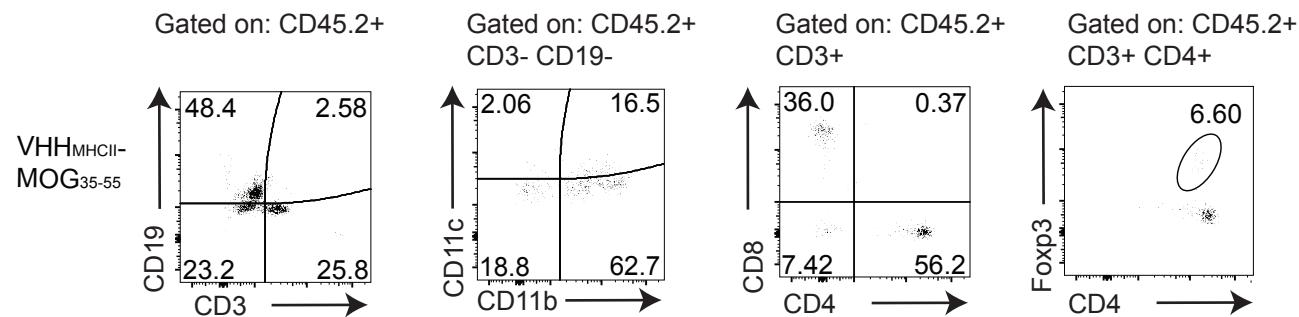
a, Individual clinical scores of mice that received splenocytes and peripheral blood mononuclear cells (PBMCs) from donor mice that have been treated with VHH$_{MHCII}$-OVA$_{323-339}$ or with VHH$_{MHCII}$-MOG$_{35-55}$. Clinical scores: 1, limp tail; 2, partial hind leg paralysis; 3, complete hind leg paralysis; 4, complete hind and partial front leg paralysis; and 5, moribund. ***p<0.001, two-way analysis of variance (ANOVA) with repeated measures. Composition of transferred splenocytes (**b**) and PBMCs (**c**) from experimental set up in (**a**).

Extended Data Figure 9
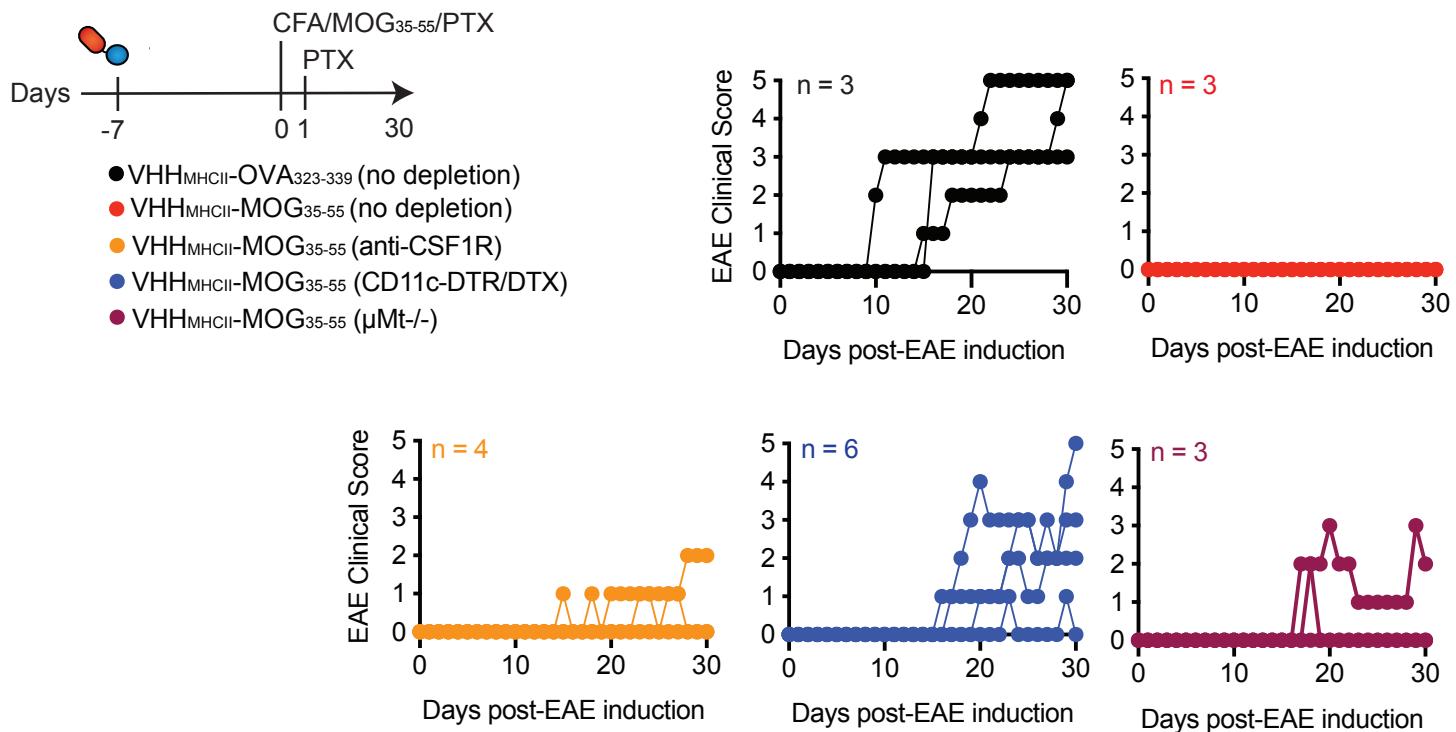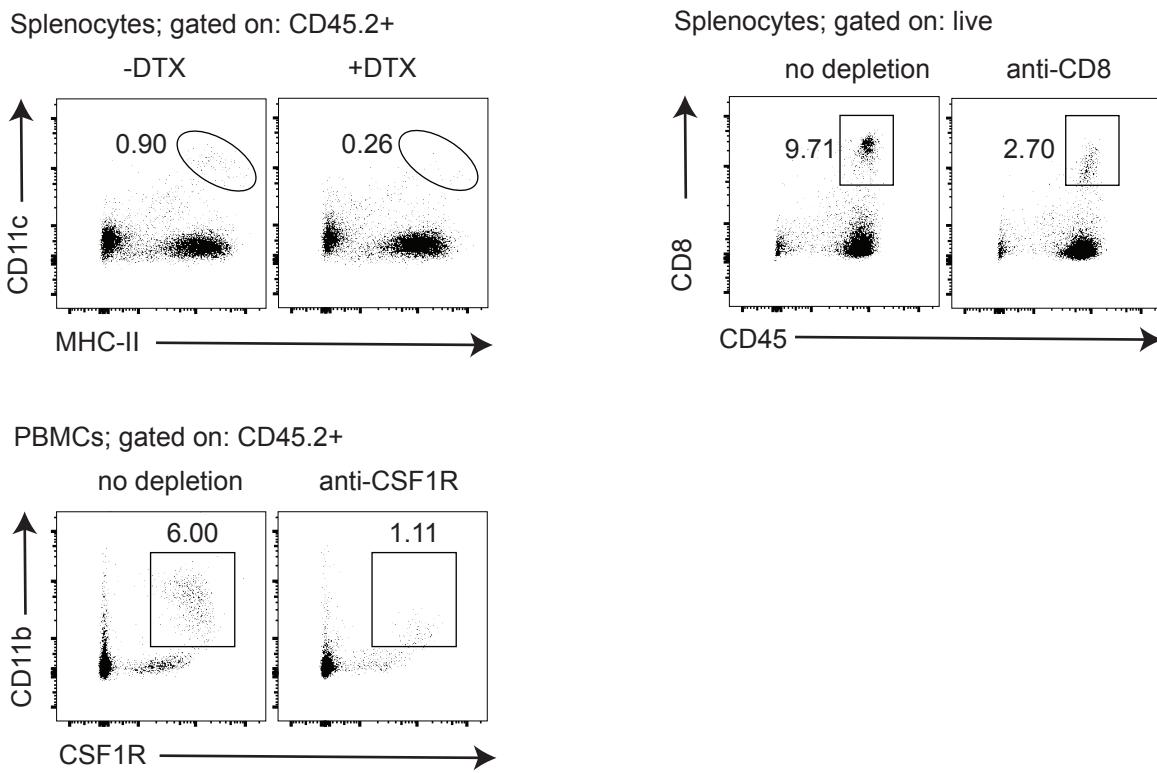
Depletion of selected cellular subsets to decipher cellular subsets that support VHH$_{MHCII}$-mediated antigen-specific tolerance.
a, Individual clinical scores of mice that received VHH$_{MHCII}$-OVA$_{323-339}$ or with VHH$_{MHCII}$-MOG$_{35-55}$ prophylactic treatment with the indicated cell subset depletion. To deplete CD8+ T cells, mice were injected with 400μg intraperitoneally (i.p.) twice weekly beginning 2 weeks prior to VHH-antigen administration and throughout the EAE observation window. Macrophages was depleted by i.p. injection of 300μg of anti-CSF1R every other day beginning beginning 2 weeks prior to VHH-antigen administration and throughout the EAE observation window. Finally, to deplete DCs, we administered a single dose of 100ng DTX i.p. into CD11c-DTR mice 2 days prior to VHH-antigen administration. **b**, Flow cytometry confirmation of the depletions of CD8+ T cells, macrophages and DCs a day prior to VHH-antigen administration.

Extended Data Figure 10
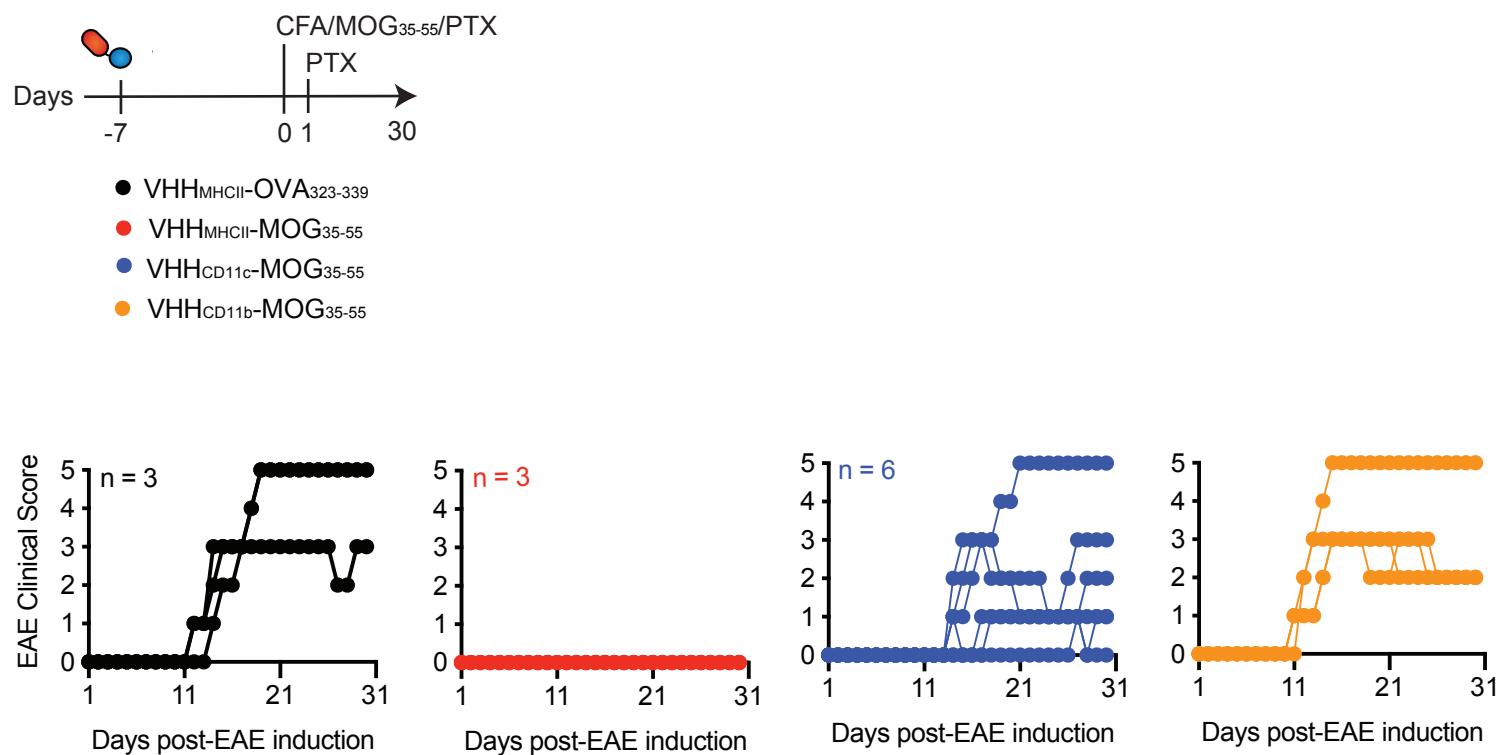
Individual clinical scores of mice that received the designated VHH-antigen. Clinical scores: 1, limp tail; 2, partial hind leg paralysis; 3, complete hind leg paralysis; 4, complete hind and partial front leg paralysis; and 5, moribund. ***p<0.001, two-way analysis of variance (ANOVA) with repeated measures.

Extended Data Figure 11
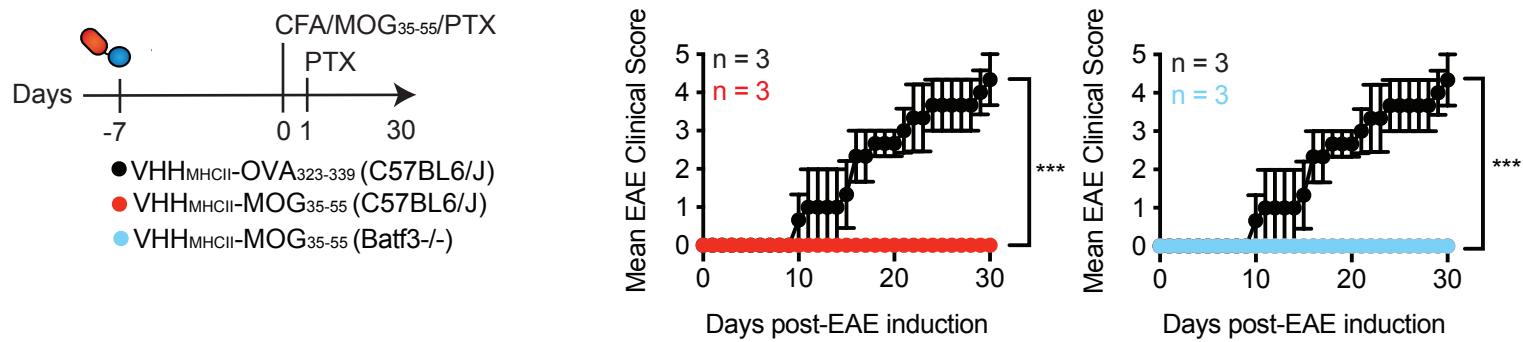
Mean clinical scores of wild type C57BL6/J or Batf3-/- mice (mice lacking CD8α+ DCs) that received the designated VHH-antigen. Clinical scores: 1, limp tail; 2, partial hind leg paralysis; 3, complete hind leg paralysis; 4, complete hind and partial front leg paralysis; and 5, moribund. ***p<0.001, two-way analysis of variance (ANOVA) with repeated measures.

Extended Data Figure 12
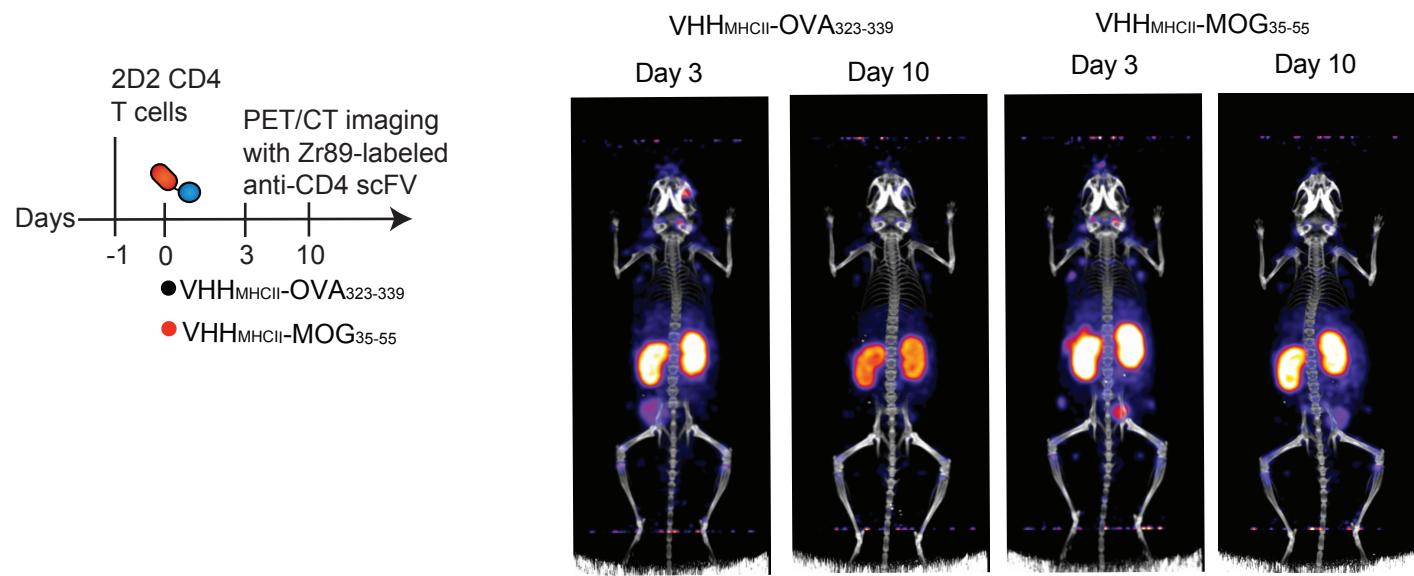
Non-invasive positron-emission tomography (PET)-CT imaging of adoptively transferred 2D2 CD4 T cells in Rag1-/- mice. In brief, 2D2 CD4 T cells were adoptively transferred into Rag1-/- mice and a day later, we administered VHH-antigen. At day 3 and 10, we injected 89Zr-labeled PEGylated anti-CD4 scFV to track the in vivo distribution of the 2D2 CD4 T cells in the whole body of the recipient mice. This representative PET-CT images corroborate our findings in Fig. 3a.

Extended Data Figure 13

a

CellTrace Violet-stained
2D2 CD4 T cells

harvest spleen

Days

-1   0   3

● VHH$_{MHCII}$-OVA$_{323-339}$
● VHH$_{MHCII}$-MOG$_{35-55}$
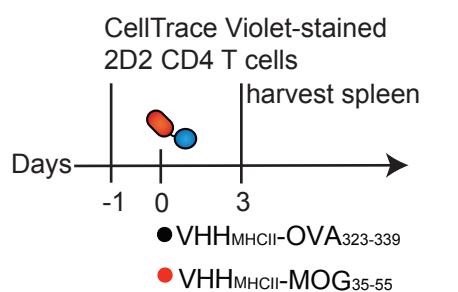
Number of division: 6 5 4 3 2 1 0

VHH$_{MHCII}$-OVA$_{323-339}$

VHH$_{MHCII}$-MOG$_{35-55}$

Violet CellTrace

b

PC2: 21% variance

PC1: 66% variance

● VHH$_{MHCII}$-OVA$_{323-339}$ ● VHH$_{MHCII}$-MOG$_{35-55}$ (div 3)   ● VHH$_{MHCII}$-MOG$_{35-55}$ (div 4)   ● VHH$_{MHCII}$-MOG$_{35-55}$ (div 5)   ● VHH$_{MHCII}$-MOG$_{35-55}$ (div 6)

c

VHH$_{MHCII}$-OVA$_{323-339}$ VHH$_{MHCII}$-MOG$_{35-55}$

\# of division: 0 0 3 3 4 4 5 5 6 6

Egr2, Ezh2, Hivep3, Ikzf2, Irf4, Irf8, Myb, Nr4a2, Nr4a3, Pou2af1, Tox, Zbtb32
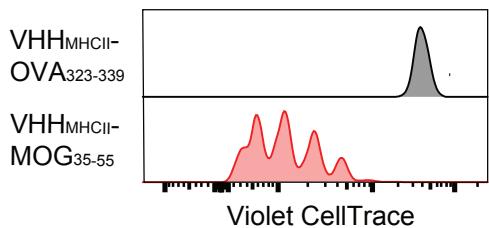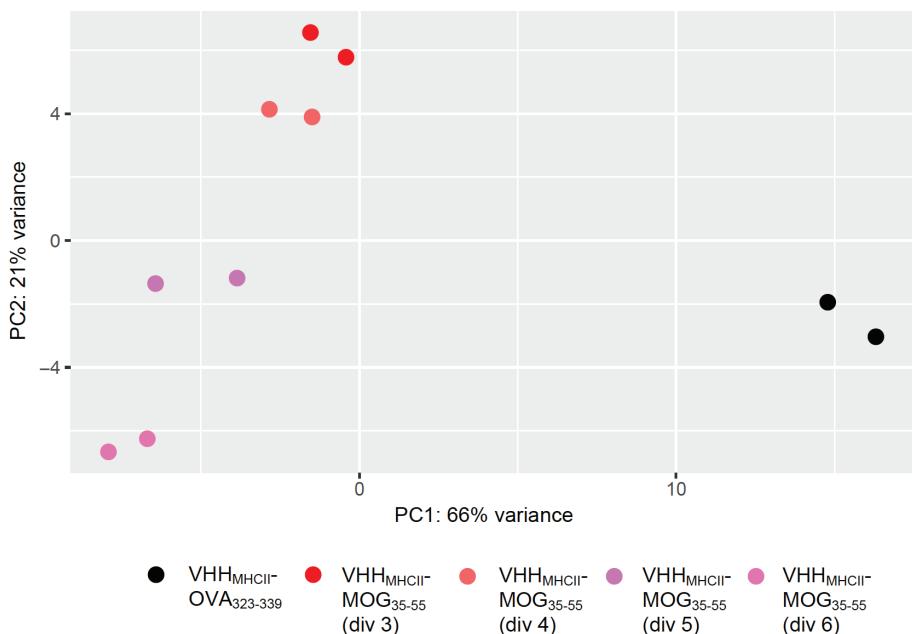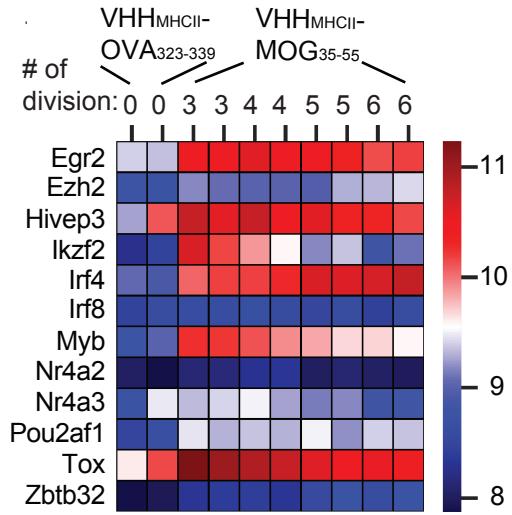
d

| GO Term	Description	P-value
GO:0002682	regulation of immune system process	4.60E-12
GO:0002376	immune system process	9.30E-12
GO:0050863	regulation of T cell activation	1.56E-11
GO:0050865	regulation of cell activation	2.79E-11
GO:0022407	regulation of cell-cell adhesion	7.83E-11
GO:0051239	regulation of multicellular organismal process	2.41E-10
GO:0030155	regulation of cell adhesion	8.42E-10
GO:1903037	regulation of leukocyte cell-cell adhesion	9.24E-10
GO:0051249	regulation of lymphocyte activation	1.06E-09
GO:0002694	regulation of leukocyte activation	1.79E-09
GO:0045321	leukocyte activation	3.94E-09
GO:0048583	regulation of response to stimulus	4.02E-09
GO:0001775	cell activation	5.32E-09
GO:0048585	negative regulation of response to stimulus	1.98E-08
GO:0042129	regulation of T cell proliferation	1.27E-07

e

GO Term	Description	P-value
GO:0043604	amide biosynthetic process	5.83E-10
GO:0043603	cellular amide metabolic process	8.43E-09
GO:1901566	organonitrogen compound biosynthetic process	3.50E-08
GO:0043043	peptide biosynthetic process	1.49E-07
GO:0006412	translation	5.92E-07
GO:0044271	cellular nitrogen compound biosynthetic process	1.01E-06
GO:0022613	ribonucleoprotein complex biogenesis	1.03E-06
GO:0006364	rRNA processing	2.20E-06
GO:0006518	peptide metabolic process	2.77E-06
GO:0044085	cellular component biogenesis	4.59E-06
GO:0016072	rRNA metabolic process	1.19E-05
GO:0002181	cytoplasmic translation	1.35E-05
GO:0034645	cellular macromolecule biosynthetic process	1.79E-05
GO:0044249	cellular biosynthetic process	2.59E-05
GO:0009058	biosynthetic process	3.90E-05

a, CellTrace Violet-labeled 2D2 CD4 T cells were adoptively transferred into congenically marked CD45.1 mice a day prior to infusion of VHH$_{MHCII}$-OVA$_{323-339}$ or VHH$_{MHCII}$-MOG$_{35-55}$. At day 3 post infusion, spleens were collected and CD45.2+ CD4+ TCRa3.2+ TCRb11+ cells were sorted and as indicated and processed for bulk transcriptomic analyses by RNAseq. **b**, Principal-components plots of RNA-seq data colored by FACS-sorted populations. Color code indicated below. **c**, Heatmap showing some transcriptional features of CD4+ T cells. Gene ontology analyses of the top 500 genes that are upregulated (**d**) and downregulated (**e**) in 2D2 CD4 T cells in mice that received VHH$_{MHCII}$-MOG$_{35-55}$ after 3 division (div 3) as compared to 2D2 CD4 T derived from mice that received VHH$_{MHCII}$-OVA$_{323-339}$.

Extended Data Figure 14
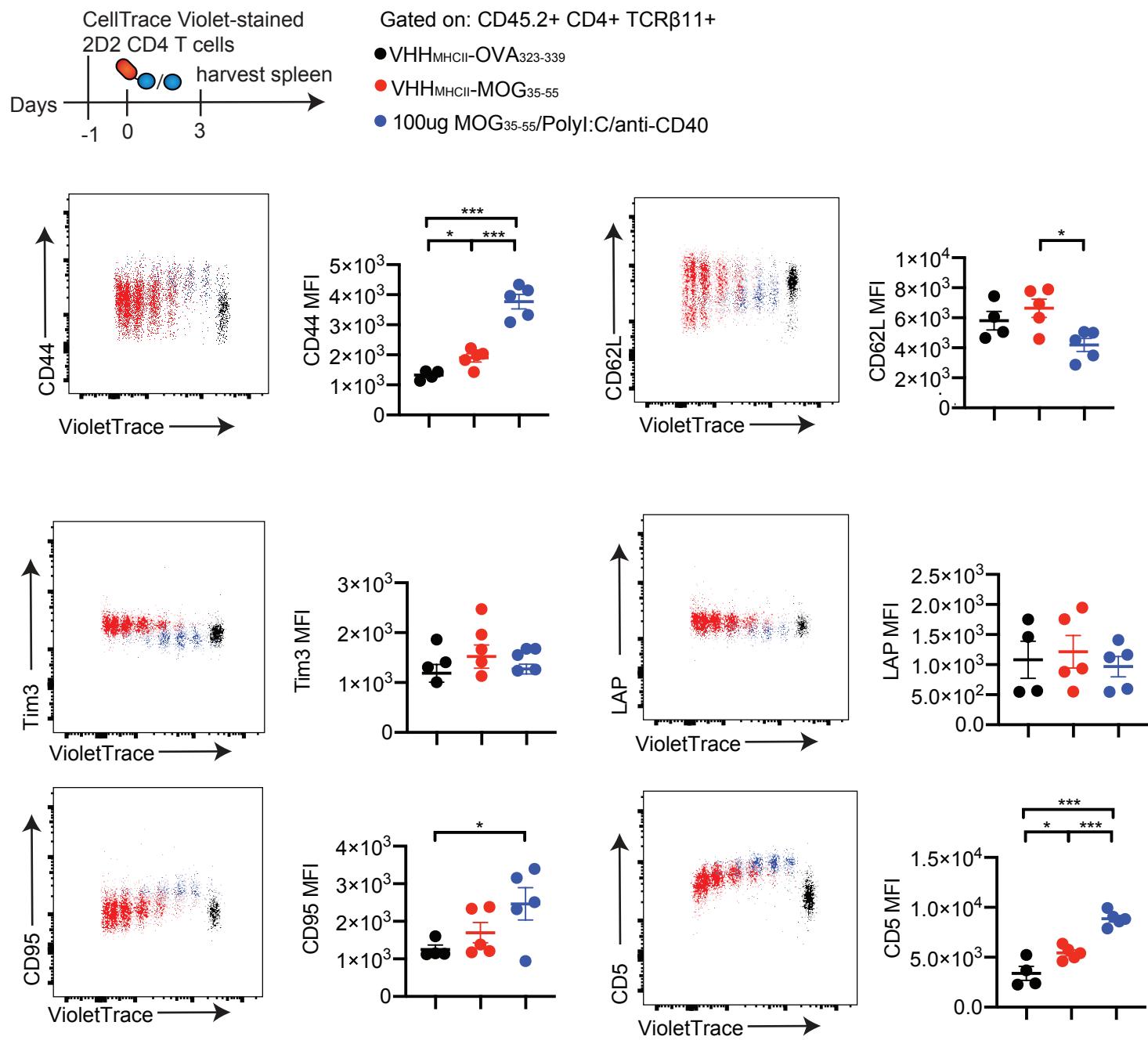
CellTrace Violet-stained 2D2 CD4 T cells

harvest spleen

Days

-1 0 3

Gated on: CD45.2+ CD4+ TCRβ11+

● VHH$_{MHCII}$-OVA$_{323-339}$
● VHH$_{MHCII}$-MOG$_{35-55}$
● 100ug MOG$_{35-55}$/PolyI:C/anti-CD40

CellTrace Violet-labeled 2D2 CD4 T cells were adoptively transferred into congenically marked CD45.1 mice a day prior to infusion of VHH$_{MHCII}$-MOG$_{35-55}$, VHH$_{MHCII}$-OVA$_{323-339}$, or equimolar MOG$_{35-55}$ peptides in the presence of PolyI:C/anti-CD40 as adjuvant. At day 3 post infusion, spleens were collected and analyzed by flow cytometry. CellTrace Violet-dilution indicates the proliferation of 2D2 T cells at day 3. VHH$_{MHCII}$-MOG$_{35-55}$ administration leads to a distinct pattern of phenotypic markers on 2D2 CD4 T cell. Representative flow images are shown and the mean fluorescent intensity (MFI) of each marker is plot as mean ± SEM. *p<0.05, ***p<0.001, unpaired t test with Holm-Sidak adjustment.

Extended Data Figure 15

a

VHH_{MHCII}-OVA_{323-339} (no depletion)
VHH_{MHCII}-MOG_{35-55} (no depletion)
VHH_{MHCII}-MOG_{35-55} (FoxP3-DTR/DTX)

b

Gated on: CD45.2+ CD3+

c

2D2 CD4 T cells



VHH_{MHCII}-OVA_{323-339}
VHH_{MHCII}-MOG_{35-55}
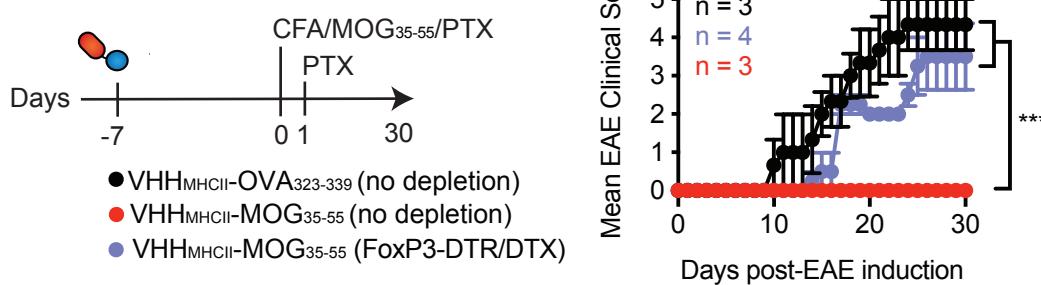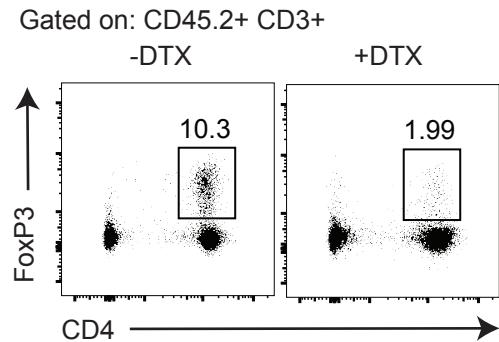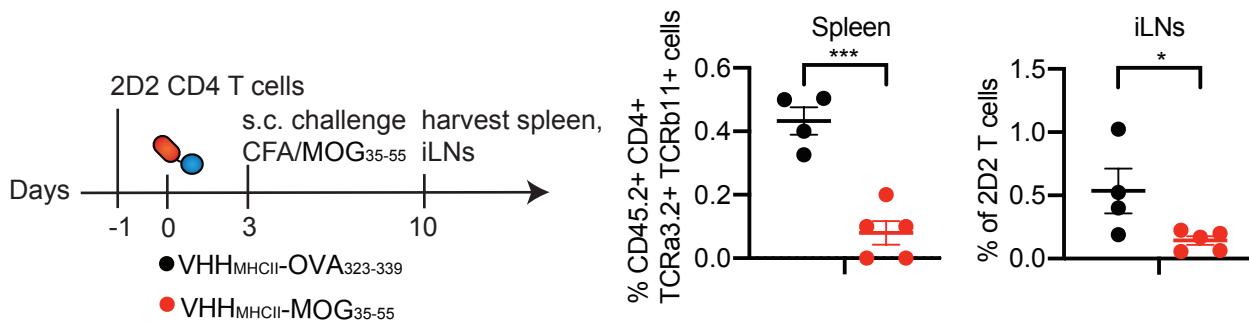
d
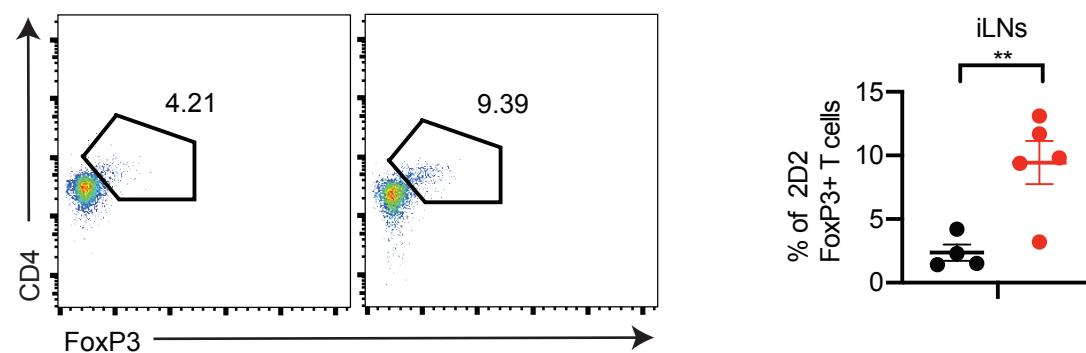
a, Mean clinical scores of mice that received VHH-peptide prophylactic treatment with or without depletion of regulatory T cells (Tregs). Tregs were depleted in FoxP3-DTR mice by injecting 3 doses of 1ug DTX i.p. at day -9, -8, -1 prior to therapy and weekly afterwards at 1ug i.p. until end point. Clinical scores: 1, limp tail; 2, partial hind leg paralysis; 3, complete hind leg paralysis; 4, complete hind and partial front leg paralysis; and 5, moribund. ***, p<0.001, two-way analysis of variance (ANOVA) with repeated measures. **b**, Flow cytometry confirmation of the depletions of FoxP3+ Tregs cells, a day prior to VHH-antigen administration. **c**, 2D2 CD4 T cells were adoptively transferred into congenically marked CD45.1 mice a day prior to infusion of VHH-antigen. We further challenged these mice with MOG_{35-55} emulsified in CFA at day 3. Spleens and iLNs were collected 7 days later. We found that 2D2 T cells in mice infused with VHH_{MHCII}-MOG_{35-55} failed to proliferate as effectively as 2D2 T cells in mice that received VHH_{MHCII}-OVA_{323-339}. Data are shown as mean ± SEM. *p<0.05, ***p<0.001, unpaired t test with Holm-Sidak adjustment. **d**, Yet, among the 2D2 T cells, we noticed an increase of FoxP3+ cells. Data are shown as mean ± SEM. **p<0.01, unpaired t test with Holm-Sidak adjustment.

Extended Data Figure 16

a
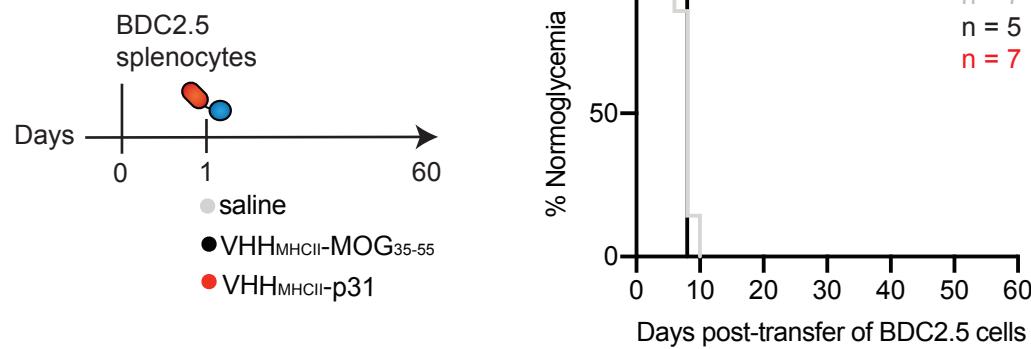
b
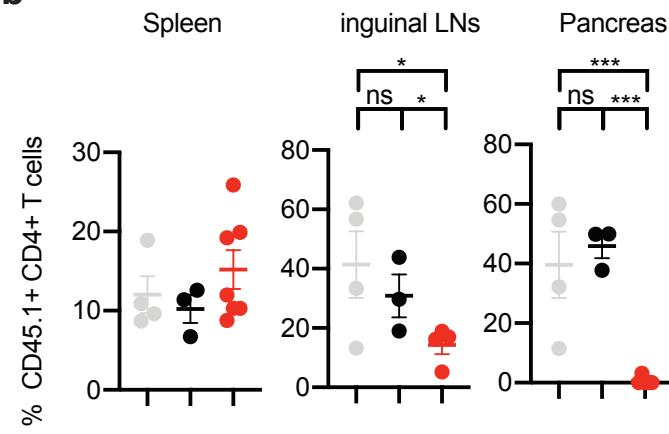
c
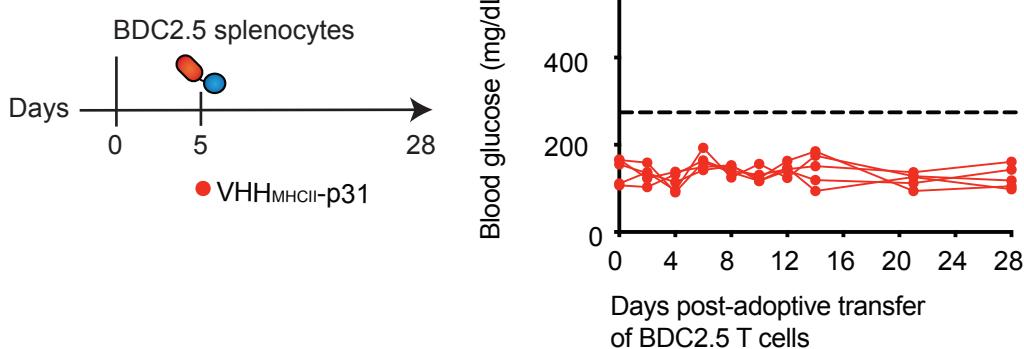
VHH$_{MHCII}$-p31 could prevent T1D. **a**, Schematic for prophylactic T1D treatment at day 1 post-adoptive transfer of activated BDC2.5 splenocytes. Overall normoglycemic percentage of the data in Fig. 4a. p<0.001, log-rank test. **b**, Flow cytometry analyses of infiltrating BDC2.5 CD4+ T cells in the designated organs 14 days after adoptive transfer of BDC2.5 splenocytes. Data shown as mean +/- SEM. n.s. not significant; *p<0.05, ***p<0.001, unpaired t test with Holm-Sidak adjustment. **c**, Schematic for semi-therapeutic T1D treatment at day 5 post-adoptive transfer of activated BDC2.5 splenocytes. Blood glucose levels were measured to monitor T1D progression. Mice were considered diabetic when glucose levels were >250 mg/dL.

Extended Data Figure 17

a

Th1 DO10.11 splenocytes

CFA/OVA s.c.   HAO challenge

Days

-11 -10.5 -10   0   7

● VHH$_{MHCII}$-OVA$_{323-339}$
● VHH$_{MHCII}$-MOG$_{35-55}$

n = 6
n = 6

Paw thickness (mm)

Days post-HOA injection

b

VHH$_{MHCII}$-MOG$_{35-55}$ VHH$_{MHCII}$-OVA$_{323-339}$

c

popliteal LNs

IFNγ (pg/mL)

OVA :   -   +   -   +

d

OD 450nm (a.u.)

Serum dilution

e

OD 450nm (a.u.)

Serum dilution
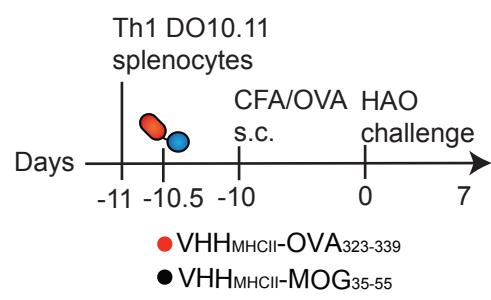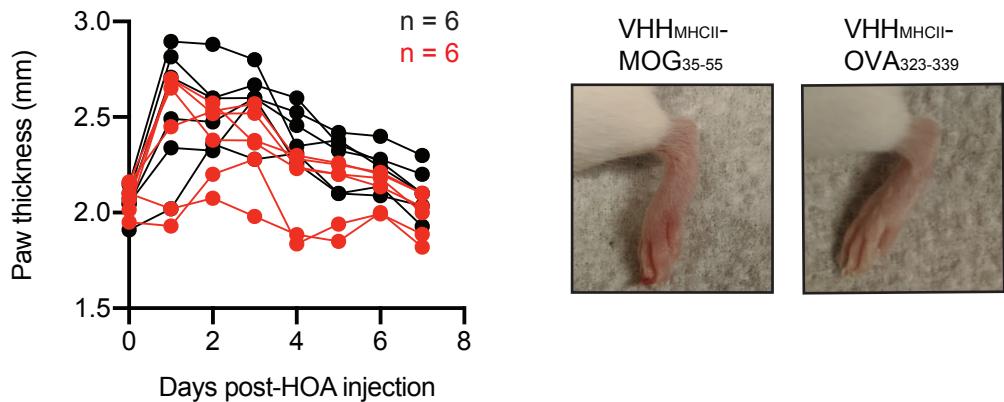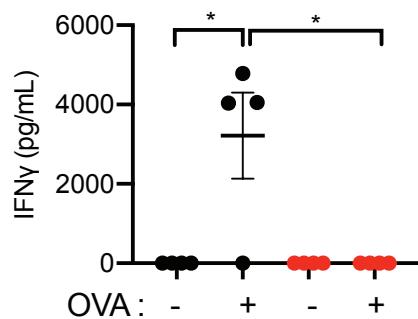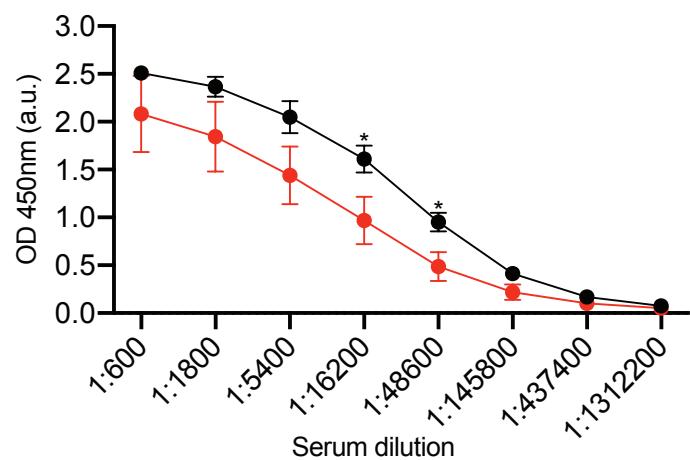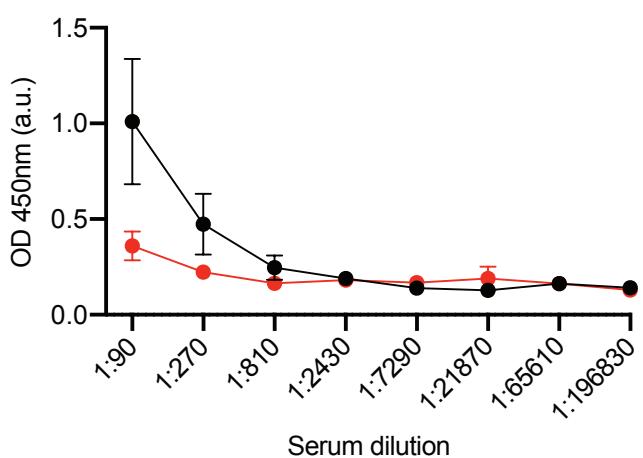
VHH$_{MHCII}$-OVA$_{323-339}$ could reduce RA severity. **a**, Individual paw thickness of the mice treated with VHH-antigens to assess RA progression. **b**, Representative images of the mouse' paw at day 3 post heat-aggregated ovalbumin (HAO) challenge. **c**, Th1 responses of popliteal lymph nodes-derived splenocytes harvested at end point (day 7 post HAO challenges). Data shown as mean +/- SEM. *$p<0.05$, unpaired t test with Holm-Sidak adjustment. Anti-Ovalbumin (**d**) and anti-OVA$_{323-339}$ (**e**) antibody responses from the mice described in (**a**). Data shown as mean +/- SEM. *$p<0.05$, unpaired t test with Holm-Sidak adjustment.

Extended Data Figure 18
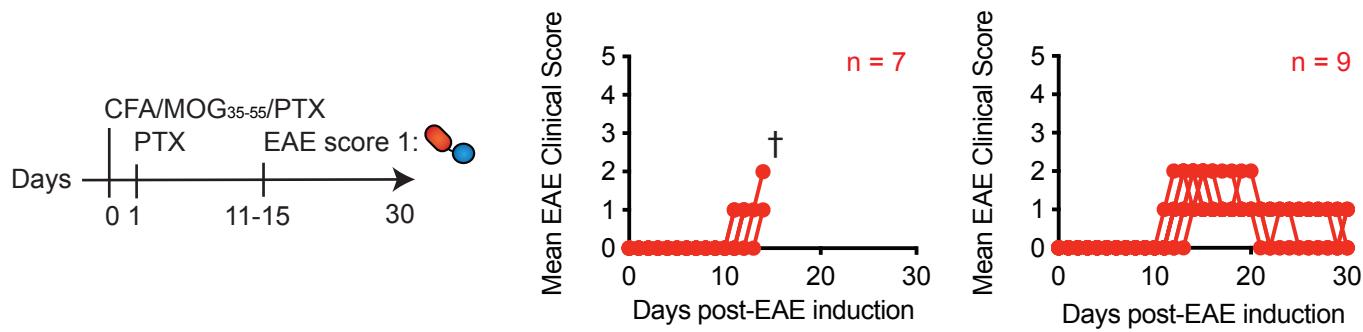
Individual clinical score of mice that were treated with a dose of received VHH_{MHCII}-MOG_{35-55} on the day the mouse reached clinical score of 1. Clinical scores: 1, limp tail; 2, partial hind leg paralysis; 3, complete hind leg paralysis; 4, complete hind and partial front leg paralysis; and 5, moribund. ~40% (7/16) of mice were found dead (†) attributed to cytokine storm.

Extended Data Figure 19
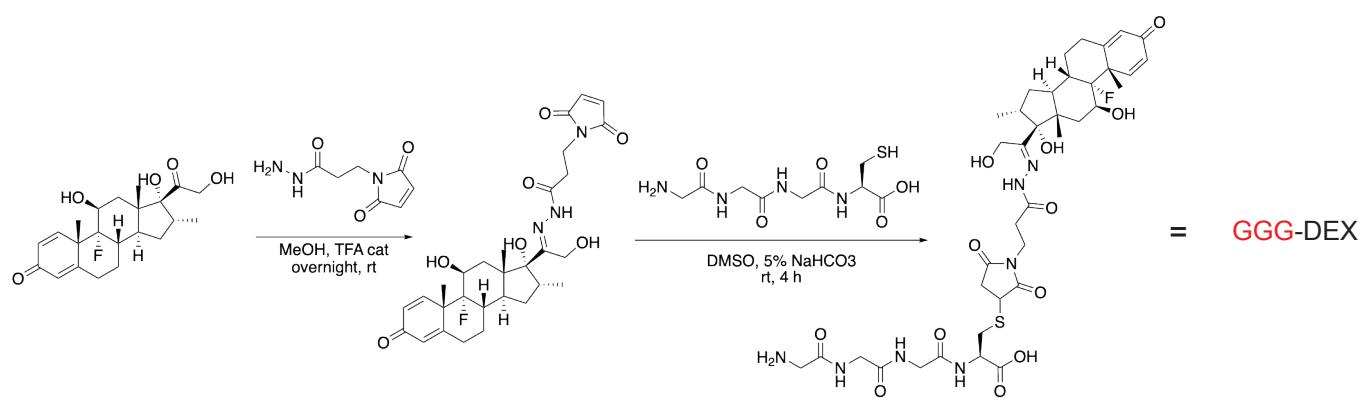
Schematic depicting the synthesis of GGG-carrying dexamethasone (DEX)

Extended Data Figure 20

a
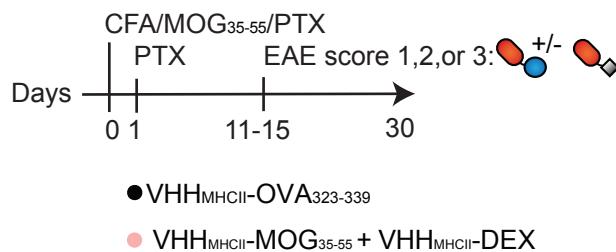
b
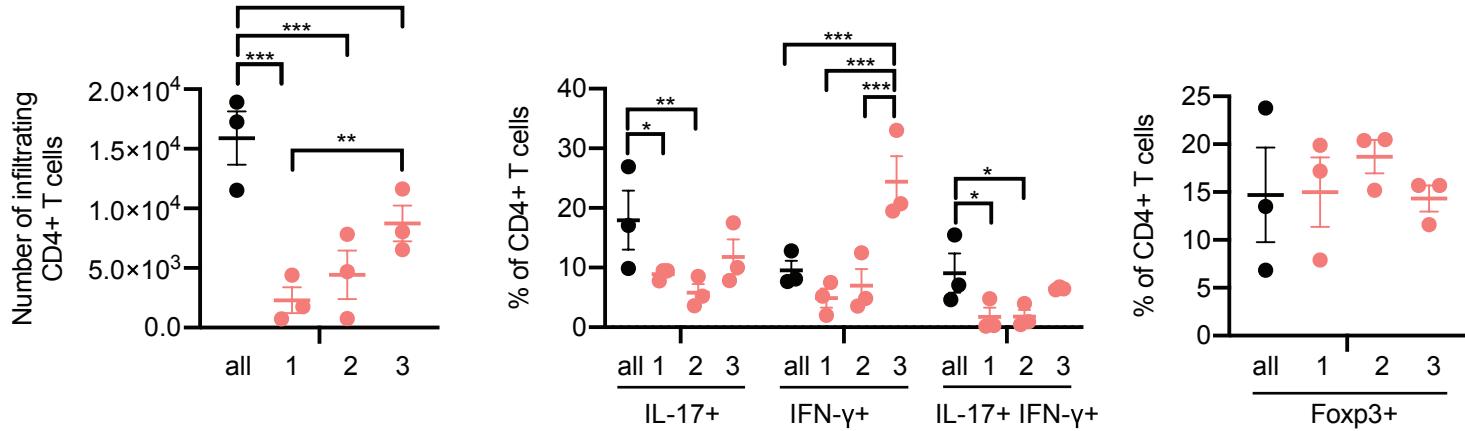
a, Experimental scheme. Clinical scores: 1, limp tail; 2, partial hind leg paralysis; 3, complete hind leg paralysis; 4, complete hind and partial front leg paralysis; and 5, moribund. **b**, Flow cytometry analyses of Th1 and Th17 infiltrating CD4+ lymphocytes in the spinal cord at the end point for each mouse described in (**a**). Frequency of FoxP3+ CD4+ regulatory T cells are also indicated. Data shown as mean +/- SEM. *p<0.05, **p<0.01, ***p<0.001, unpaired t test with Holm-Sidak adjustment.

Extended Data Figure 21

a
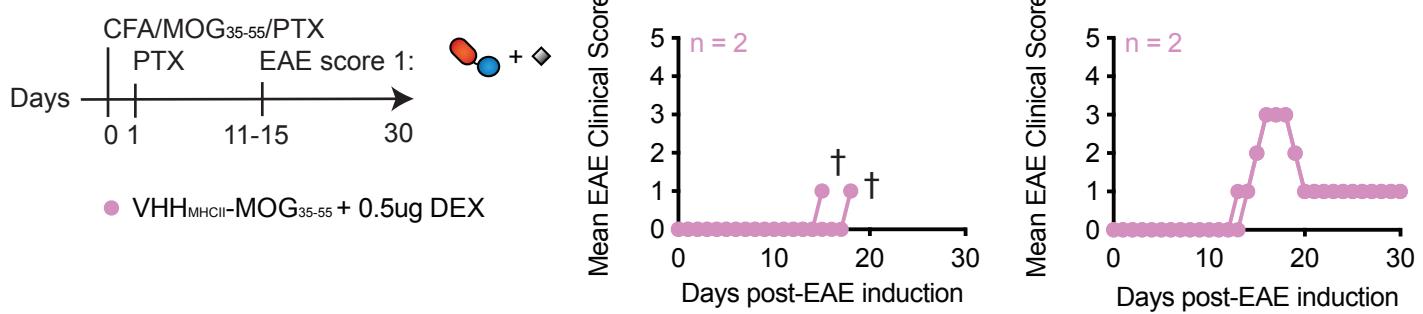
b

Individual clinical score of mice that were treated with a dose of received VHH$_{MHCII}$-MOG$_{35-55}$ in the presence 0.5ug DEX (**a**) or 100ug DEX (**b**) on the day the mouse reached clinical score of 1. Clinical scores: 1, limp tail; 2, partial hind leg paralysis; 3, complete hind leg paralysis; 4, complete hind and partial front leg paralysis; and 5, moribund. 50% (2/4) of mice were found dead (†) when they received only 0.5ug DEX attributed to cytokine storm.